PNAS RESEARCH ARTICLE | BIOCHEMISTRY

The pathway for coenzyme M biosynthesis in bacteria

Hsin-Hua Wu[a,b], Michael D. Pun[b], Courtney E. Wise[c], Bennett R. Streit[d], Florence Mus[a], Anna Berim[a], William M. Kincannon[d], Abdullah Islam[a], Sarah E. Partovi[d], David R. Gang[a], Jennifer L. DuBois[d], Carolyn E. Lubner[c], Clifford E. Berkman[b], B. Markus Lange[a,e], and John W. Peters[a,1]

Edited by John Cronan, University of Illinois at Urbana Champaign, Urbana, IL; received April 25, 2022; accepted July 27, 2022

Mercaptoethane sulfonate or coenzyme M (CoM) is the smallest known organic cofactor and is most commonly associated with the methane-forming step in all methanogenic archaea but is also associated with the anaerobic oxidation of methane to CO_2 in anaerobic methanotrophic archaea and the oxidation of short-chain alkanes in *Syntrophoarchaeum* species. It has also been found in a small number of bacteria capable of the metabolism of small organics. Although many of the steps for CoM biosynthesis in methanogenic archaea have been elucidated, a complete pathway for the biosynthesis of CoM in archaea or bacteria has not been reported. Here, we present the complete CoM biosynthesis pathway in bacteria, revealing distinct chemical steps relative to CoM biosynthesis in methanogenic archaea. The existence of different pathways represents a profound instance of convergent evolution. The five-step pathway involves the addition of sulfite, the elimination of phosphate, decarboxylation, thiolation, and the reduction to affect the sequential conversion of phosphoenolpyruvate to CoM. The salient features of the pathway demonstrate reactivities for members of large aspartase/fumarase and pyridoxal 5′-phosphate–dependent enzyme families.

Xanthobacter autotrophicus | CoM biosynthesis | aspartase/fumarase superfamily | sulfonate | PLP-dependent cysteine desulfhydrase

Significance

Coenzymes are nonprotein molecules of varying molecular weight that are required for certain enzymatic reactions where they function as carriers of functional groups or electrons and in orienting substrates appropriately relative to protein functional groups for catalysis. Coenzyme M (mercaptoethane sulfonate, CoM) is the smallest known organic coenzyme and functions in key roles in pathways for methanogenesis in archaea and in propylene metabolism in bacteria. Elucidating the pathway of CoM biosynthesis in bacteria in this work reveals that CoM is synthesized by different enzymatic transformations than those observed in methanogens from a common metabolite precursor (phosphoenolpyruvate), suggesting that the pathways in archaea and bacteria have evolved through convergent evolution.

Coenzyme M (2-mercaptoethanesulfonate; CoM) was isolated and characterized by McBride and Wolfe in the early 1970s (1) as the smallest organic cofactor and the only cofactor containing a sulfonate functional group, separated from a reactive thiol via an ethyl group linkage (2, 3). CoM is one of several unique cofactors associated with the biological reduction of CO_2 to methane in methanogenic archaea (1, 4–6), the anaerobic oxidation of methane to CO_2 in anaerobic methanotrophic archaea (7), and the oxidation of short-chain alkanes, such as propane and butane, to form CO_2 in *Syntrophoarchaeum* species (8, 9). It was thought that this cofactor was exclusively associated with methanogenesis until the late 1990s, when CoM was unexpectedly discovered to have a role in bacterial alkene metabolism in the alpha proteobacterium *Xanthobacter autotrophicus* Py2 (10, 11). This fascinating discovery revealed that both archaea and bacteria have evolved uses for CoM, where it plays a key role in promoting orientation of substrates for regiospecific and stereospecific chemistry.

In *X. autotrophicus* Py2, propylene and CO_2 are converted through a four-step pathway to acetoacetate (Fig. 1), which subsequently feeds into central metabolism. Propylene metabolism is initiated through epoxidation via an NADH-dependent alkene monooxygenase, forming an enantiomeric mixture of (*R*)- and (*S*)-epoxypropane. Subsequently, the electrophilic epoxide is opened by nucleophilic attack of the CoM thiol to form (*R*)- and (*S*)-hydroxypropyl-CoM. CoM then functions in the final two steps of the pathway to align substrates for stereospecific dehydrogenation and thiol-dependent reductive cleavage reactions. These result in the formation of the final acetoacetate product and liberate free CoM (10, 12).

Two pathways for CoM biosynthesis have been described in methanogens, where the carbon backbone for CoM is derived from either phosphoenolpyruvate (PEP) in the more deeply branching Class I methanogens or phosphoserine in Class II (Methanomicrobiales) and Class III (Methanosarcinales) methanogens (13–17) (*SI Appendix*, Fig. S1). The PEP-dependent pathway is initiated by the nucleophilic addition of sulfite to PEP, yielding (*R*)-phosphosulfolactate (PSL), in a reaction catalyzed by PSL synthase (ComA) (18, 19). PSL phosphatase (ComB) subsequently catalyzes the oxidative dephosphorylation of (*R*)-PSL, producing (*R*)-sulfolactate, which then undergoes NAD^+-dependent oxidation by the activity of sulfolactate dehydrogenase (ComC) to form sulfopyruvate (13, 15, 20, 21). Sulfopyruvate is a shared intermediate with the phosphoserine-dependent pathway in Class II methanogens, where L-phosphoserine undergoes a concerted elimination of the β-phosphate and addition of sulfite to generate L-cysteate, via the activity of a pyridoxal 5′- phosphate (PLP)-dependent cysteate

Author contributions: H.-H.W., F.M., S.E.P., J.L.D., C.E.B., and J.W.P. designed research; H.-H.W., M.D.P., C.E.W., B.R.S., F.M., A.B., W.M.K., A.I., and B.M.L. performed research; H.-H.W. and D.R.G. contributed new reagents/analytic tools; H.-H.W., M.D.P., C.E.W., B.R.S., F.M., A.B., W.M.K., J.L.D., C.E.L., and B.M.L. analyzed data; H.-H.W. and J.W.P. wrote the paper; and C.E.W., F.M., J.L.D., C.E.L., C.E.B., and B.M.L. performed writing review and editing.

The authors declare no competing interest.

This article is a PNAS Direct Submission.

[1]To whom correspondence may be addressed. Email: jw.peters@wsu.edu.

This article contains supporting information online at http://www.pnas.org/lookup/suppl/doi:10.1073/pnas.2207190119/-/DCSupplemental.

Published August 29, 2022.

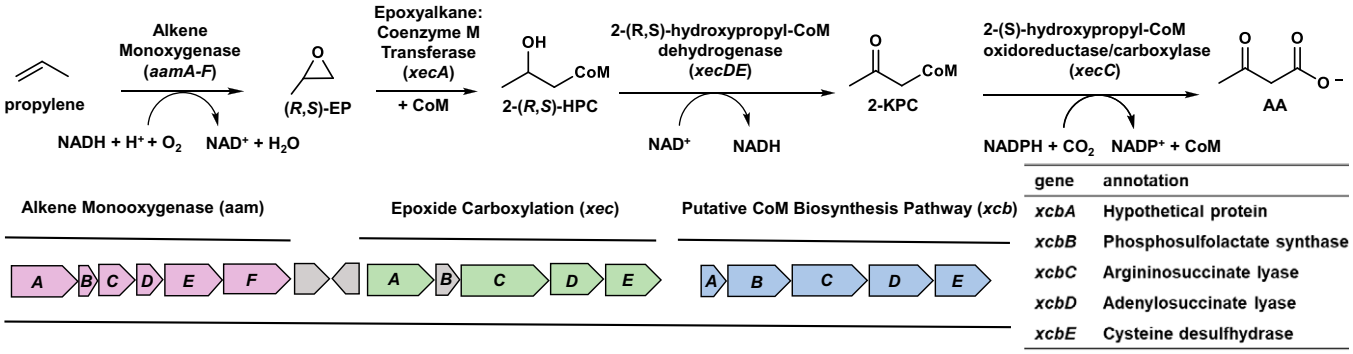

Fig. 1. Propylene metabolism in *X. autotrophicus* Py2. The identified 320-kb linear megaplasmid of *X. autotrophicys* Py2 contains the genes for propylene metabolism (*aam*, *xec* clusters) and a putative CoM biosynthetic pathway (*xcb* cluster). Gene annotations for the putative CoM biosynthetic pathway are tabulated. Genes encoding alkene monooxygenase subunits are shown in pink; the remaining four enzymes involved in converting propylene oxide to acetoacetate correspond to genes in green; the putative CoM biosynthetic gene cluster is shown in blue. Alkene-related functions for the open reading frames shown in gray have not been assigned. (*R*,*S*)-EP, (*R*)-epoxypropane, (*S*)-epoxypropane; 2-(*R*,*S*)-HPC, 2-(*R*)-hydroxypropyl-CoM, 2-(*S*)-hydroxypropyl-CoM; 2-KPC, 2-ketopropyl-CoM; AA, acetoacetate.

synthase. L-cysteate then undergoes transamination by a canonical PLP-dependent aspartate aminotransferase to form sulfopyruvate. After this, the Class I and Class II methanogenic pathways are presumed to follow the same chemical steps, in which a thiamine pyrophosphate-dependent sulfopyruvate decarboxylase (ComDE) catalyzes the decarboxylation of sulfopyruvate to form sulfoacetaldehyde. This product presumably undergoes reductive thiolation to yield CoM although this has not been confirmed biochemically.

Despite the significant scope of work on the methanoarchaeal CoM biosynthesis pathway, the CoM biosynthetic pathway in bacteria remains unclear. Analysis of the genomes of several bacteria known to possess CoM-dependent alkene metabolism allowed for the identification of genes and gene clusters that could be implicated as potentially having a role in CoM biosynthesis and the rationalization of a putative biochemical pathway (22, 23). Initially, alkene metabolism genes in *X. autotrophicus* Py2 were reported to be propylene inducible, and the synthesis of CoM coordinately regulated with the expression of alkene monooxygenase and epoxide carboxylase enzymes (24, 25). These findings suggested clustering of the respective genes under a common regulatory element identified upstream from the alkene monooxygenase translational start (21). Indeed, strains of propylene-grown *X. autotrophicus* Py2 were found to contain a single 320-kb linear megaplasmid (pXAUT01), whereas strains repeatedly cultured on other carbon sources lacked this extrachromosomal element. Investigation of the region downstream from the alkene monooxygenase and epoxide carboxylase gene clusters revealed five putative genes (*xcbA-E*) (15), of which only *xcbB* encoded a polypeptide sharing significant homology with proteins involved in CoM biosynthesis in methanogenic archaea. XcbB is a homolog of ComA, the first enzyme of the PEP-dependent CoM biosynthetic pathway in *Methanocaldococcus jannaschii* (26). The genome of *X. autotrophicus* Py2 has revealed no additional genes encoding proteins with significant similarity to either methanoarchaeal pathway, suggesting that the CoM biosynthesis pathway in bacteria has evolved separately from the one in methanogens (15).

In previous work, we confirmed that XcbB possesses PSL synthase activity (15) in support of this. Furthermore, the adjacent enzymes, XcbC and XcbD, are classified as members of aspartase/fumarase superfamily (AFS) through phylogenetic studies, with XcbC and XcbD having significant homology with arginosuccinate lyase (ASL) and adenylosuccinate lyase (ADL), respectively. AFS members are known to catalyze β-elimination reactions of succinyl-containing substrates, yielding fumarate as the common unsaturated elimination product (27, 28). We also have demonstrated that XcbC catalyzes the β-elimination of phosphate from PSL and the generation of sulfoacrylic acid (SAA), establishing a reactivity that has not been observed before for the AFS (15) (Fig. 2). In this work, we a have determined the remaining steps converting SAA to CoM thereby elucidating the full pathway for CoM biosynthesis in bacteria.

Results and Discussion

To affect the synthesis of CoM from SAA, thiolation and decarboxylation are required, and we envisioned that these transformations are accelerated by the three remaining proteins encoded in this gene cluster (XcbD, XcbE, and XcbA). As mentioned above, like XcbC, XcbD is a member of the AFS, catalyzing β-elimination/β-addition. XcbE is annotated as a PLP-dependent protein most closely related to cysteine desulfhydrase, which catalyzes the liberation of H_2S from cysteine, and XcbA is a protein of unknown function (29). Given that the XcbC reaction resulted in the β-elimination of phosphate, to generate the unsaturated SAA product, we hypothesized that the other AFS homolog XcbD could catalyze a β-addition reaction perhaps that activates SAA in some manner to facilitate decarboxylation. The homology of XcbD to adenylosuccinate lyase also suggested that the substrate for XcbD might be AMP, which would result in a product that would be in essence activated for a decarboxylation reaction with AMP as a leaving group (28). Last, since XcbE is a pyridoxal-phosphate-dependent enzyme similar to cysteine desulfhydrase, we proposed that XcbE reactivity promotes thiolation in some manner.

In order to elucidate the roles of XcbD, XcbE, and XcbA, we started to study the pathway in a stepwise fashion. Although we anticipated that the next step following the XcbC-catalyzed reaction was adenylation of the SAA via β-addition catalyzed by the ADL homolog, XcbD, we were unable to demonstrate that XcbD could catalyze this reaction. Considering the possibility that the unobservable adenylation of SAA by XcbD was an artifact of monitoring the enzyme independently, and that the pathway enzymes might function optimally in concert, we developed a single pot synthesis of CoM. This single pot synthesis included PEP and sulfite, the known substrates for the first step catalyzed by phosphosulfolactate synthase (XcbB), AMP as the cosubstrate for XcbD, and cysteine as the cosubstrate for XcbE and a precursor for the CoM thiol. Incubating this group of substrates with the suite of enzymes XcbA, XcbB, XcbC, XcbD, and XcbE indeed yielded CoM, which was first derivatized by phthalaldehyde and

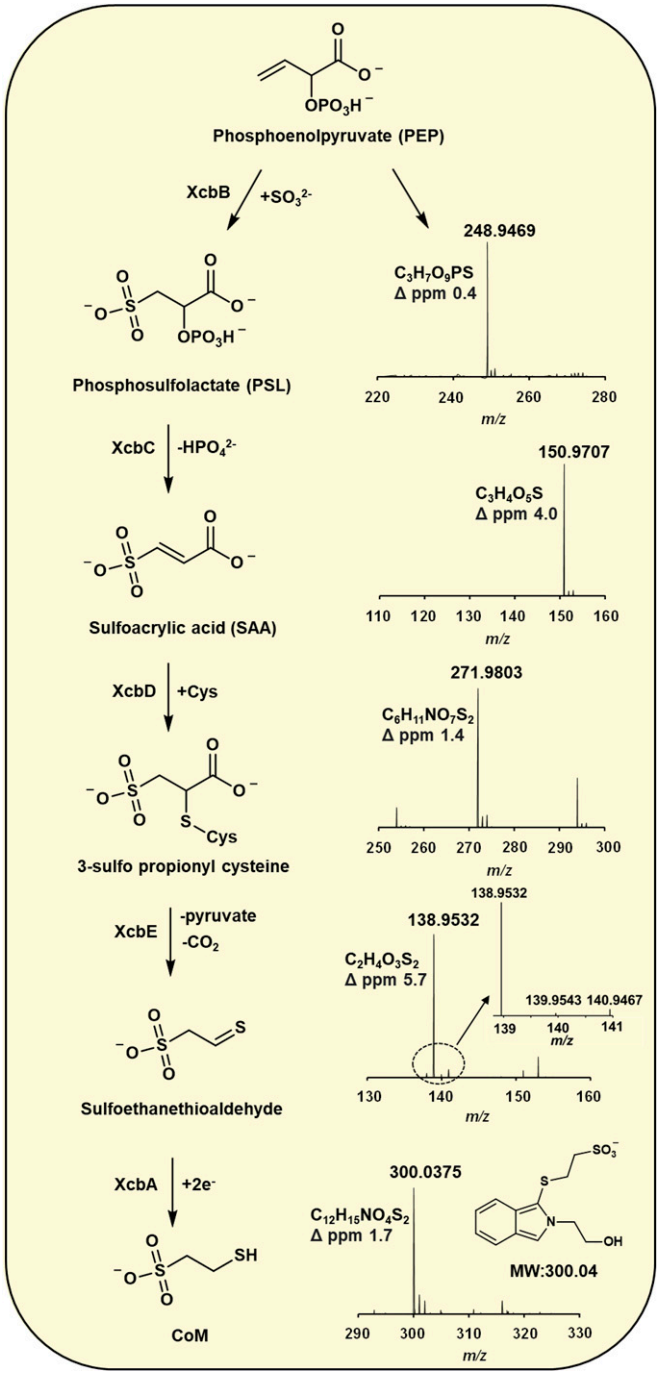

Fig. 2. Elucidation of the complete CoM biosynthetic pathway in bacteria. The conversion of PEP to CoM was catalyzed by XcbA-E and monitored via the mass spectrometry. The products of each enzymatic reaction are shown on the left with mass spectra for each product shown on the right. The mass errors are indicated as delta part-per-million (ppm) in each spectrum along with the corresponding chemical formula. The *Inset* with magnified view of mass spectra represents the isotope distribution of sulfoethanethioaldehyde. The *Inset* chemical structure in the final step of mass spectrometry data represents the derivatized CoM by using phthalaldehyde and ethanolamine. For clarity, protonation steps are omitted.

ethanolamine and then detected using high-performance liquid chromatography-quadrupole time of flight-mass spectrometry (HPLC-QTOF-MS). The single pot reaction also accumulated anticipated intermediates including SAA but we were unable to identify an intermediate consistent with the adenylation of SAA. We did, however, unexpectedly observe a mass spectrometric signal at 271.9803 *m/z* ($[M-H]^-$-species, negative ion mode) matching the expected *m/z* value for the molecular formula of a SAA–cysteine conjugate, 3-sulfo propionyl cysteine (3-SPC) ($C_6H_{11}NO_7S_2$ for the undissociated form). We then examined the reaction in a single enzyme reaction including XcbD with SAA and cysteine as substrates and the product by mass spectrometry (Fig. 2). The structure was further confirmed by tandem MS with a series of fragments including 253.9794 *m/z* (loss of water) and 190.0182 *m/z* (loss of sulfonate) (*SI Appendix*, Fig. S2), for example. To further investigate the reaction, time-resolved ^{1}H NMR was used to monitor the conversion of SAA to 3-SPC, by XcbD in real time. The pair of characteristic doublets of SAA (6.96/6.93 and 6.53/6.50 ppm) showed clear signs of consumption in the presence of XcbD and cysteine. Meanwhile, the production of 3-SPC was detected by increased intensity of a pair of a pair of doublets of doublets signals upfield (centered at 3.24/3.23 and 3.22/3.21 ppm) and a doublet signal (centered at 3.05/3.04) (Fig. 3). The reaction catalyzed by XcbD is unique in the AFS family and expands the integration of cysteine to new metabolic processes while advancing the goal of elucidating the CoM biosynthesis pathway in bacteria.

The 3-SPC product itself is a good substrate candidate for the downstream PLP-dependent XcbE enzyme. Select PLP-dependent enzymes have been shown to catalyze decarboxylation reactions by formation of an external aldimine or Schiff base linkages with PLP via the amino functional group of an amine substrate. The decarboxylation reaction is initiated by the loss of CO_2 and forms an α-carbanionic PLP intermediate. This intermediate is delocalized and stabilized by the conjugated π-bonding system of PLP and results in the quinonoid intermediate, followed by the protonation of the intermediate at the Cα to produce an amine (30).

For the XcbE catalyzed reaction, we hypothesized that the amino group of 3-SPC could form an aldimine with PLP and facilitate a decarboxylation reaction, resulting in the formation of the product sulfoethanethioaldehyde and either alanine or pyruvate + ammonia. The XcbE-catalyzed reaction was initially monitored by time-resolved ^{1}H NMR with the addition of XcbE enzyme and the filtrate from XcbD reaction, where a decrease in the doublet signal of 3-SPC was accompanied by an increase in the singlet signal (3.18 ppm) presumably indicating the production of sulfoethanethioaldehyde (Fig. 3 and *SI Appendix*, Fig. S3 contains more detailed control experiments). The doublet of doublet pattern of 3-SPC is not visible in Fig. 3*C* as a likely result of the addition of H_2O when the XcbE enzyme was added or precipitation of reaction components resulting in lowering of the J-coupling and/or signal broadening as observed previously (31–33). In addition, since we did not lock and shim the sample after the addition of the XcbE enzyme to preserve parameters, the addition of XcbE enzyme could result in a minor change in the lock signal and this could be another contribution to the loss of resolution in Fig. 3*C*.

Since the overlap of the singlet signal with the doublet from the 3-SPC somewhat obscured an unambiguous determination, we confirmed the formation of sulfoethanethioaldehyde by HPLC-QTOF-MS. Sulfoethanethioaldehyde is a well-characterized compound and known to be unstable (34), however, we were able to detect a signal at 138.9532 *m/z* in negative mode that was consistent with the expected $[M-H]^-$ signal of sulfoethanethioaldehyde based on the molecular formula ($C_2H_4O_3S_2$ for the undissociated form). In support of this assignment, stable isotopes, ^{34}S (4.2%), ^{33}S (0.75%), and ^{36}S (0.015%) are observed in the MS data, where 140.9467 (^{34}S-species) is more abundant than 139.9543 (^{33}S-species) (Fig. 2).

To complete the synthesis of CoM, reduction of sulfoethanethioaldehyde is required as a final step. XcbA was not found to

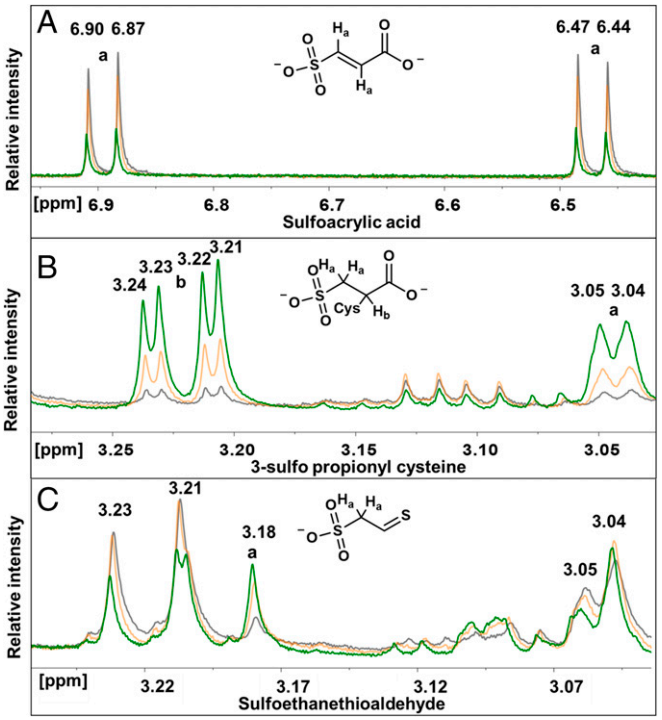

Fig. 3. Time-resolved ^{1}H NMR showed consumption of (*A*) sulfoacrylic acid (SAA) to (*B*) 3-sulfo propionyl cysteine by the XcbD reaction. (*C*) Sulfoethanethioaldehyde acid was produced by the incubation of XcbE and 3-sulfo propionyl cysteine. The signal (a and b) that represents respective protons are labeled in *A*–*C*. For clarity, only three time points are shown (gray, 0–2 min; orange, 28–30 min; green, 58–60 min).

homologous to any known protein, but we were able to purify the protein and noted it had a reddish-brown hue. The ultraviolet/visible absorbance spectrum of XcbA revealed bands with relative maxima at 420, 460, and 550 nm (Fig. 4). These absorbances decreased with added sodium dithionite as a reductant, suggesting the chromophore was redox-active (35). Further characterization using electron paramagnetic spectroscopy revealed a rhombic signal with *g*-values at 1.89, 1.96, and 2.03 consistent with a reduction-dependent $[2Fe\text{-}2S]^{1+}$ cluster (Fig. 4) (36). The sequence of XcbA contains nine cysteine residues, although no conserved motifs were observed that would be strongly indicative of either previously observed [FeS] cluster binding or catalytic cysteine disulfide. To further confirm the ability of XcbA to participate in an oxidation-reduction reaction, the reduction potential of XcbA was measured at -372 ± 4 mV versus SHE using square wave voltammetry (*SI Appendix*, Fig. S4). The addition of XcbA in a reaction including filtrate from XcbE reaction resulted in the formation of CoM detected by derivatization using phthalaldehyde and ethanolamine, with subsequent quantitation of the resulting fluorescent CoM derivative. The production of CoM was then further confirmed by HPLC-QTOF-MS in negative mode whereby the $[M\text{-}H]^{-}$ signal at 300.0375 Da matched the expected *m/z* based on the molecular formula of derivatized CoM ($C_{12}H_{15}NO_4S_2$ for the undissociated form) (Fig. 2). Interestingly, the XcbA catalyzed reduction can be accomplished in the single pot reaction without added reducing agents. We have attempted to reduce purified XcbA directly with cysteine, a two-electron reductant; however, we were unable to detect complete reduction based on the lack of appearance of the $[2Fe\text{-}2S]^{1+}$ rhombic EPR signal that is observed upon reduction with a one-electron reductant, sodium dithionite (Fig. 4). This suggests that the [Fe-S] cluster XcbA is capable of storing only one of the two reducing equivalents necessary for the CoM-generating reduction of the thioaldehyde substrate. The fact that cysteine is a catalytically competent reductant suggests that the one-electron $[2Fe\text{-}2S]^{2+/1+}$ redox couple can be bypassed by an appropriate two electron donating thiolate reductant. Pathways involving [FeS]-cluster mediated delivery of two electrons in rapid sequence, as well as direct reduction of an XcbA-associated cysteine disulfide through mixed disulfide intermediates, could both be operational (*SI Appendix*, Fig. S13). This arrangement, which would allow for flexible use of available reducing equivalents, is in some ways reminiscent of ferredoxin-thioredoxin reductase systems (37).

In summary, our previous studies have demonstrated that XcbB catalyzes sulfite addition to PEP, thus producing PSL. Bioinformatics results suggested only XcbB is homologous to a known CoM-producing enzyme, namely ComA, which catalyzes the first step of PEP-dependent CoM biosynthesis in methanogens. This indicates that the bacterial CoM biosynthesis pathway is distinct from the pathway in methanogens. The following enzyme in the bacteria pathway, XcbC, is an AFS family enzyme that has been shown to catalyze a unique α,β-elimination reaction of phosphate from PSL to produce SAA. Those results constituted an important milestone toward elucidating the entire CoM biosynthesis pathway. Although XcbD is identified as an AFS family enzyme and is closest to ADL, the enzyme uses cysteine as a cosubstrate to form 3-sulfo propionyl cysteine as a resulting product. To our knowledge, this reaction has not been observed before in AFS family enzymes. The resulting product is then acted on by the PLP-dependent XcbE enzyme where the formation of an

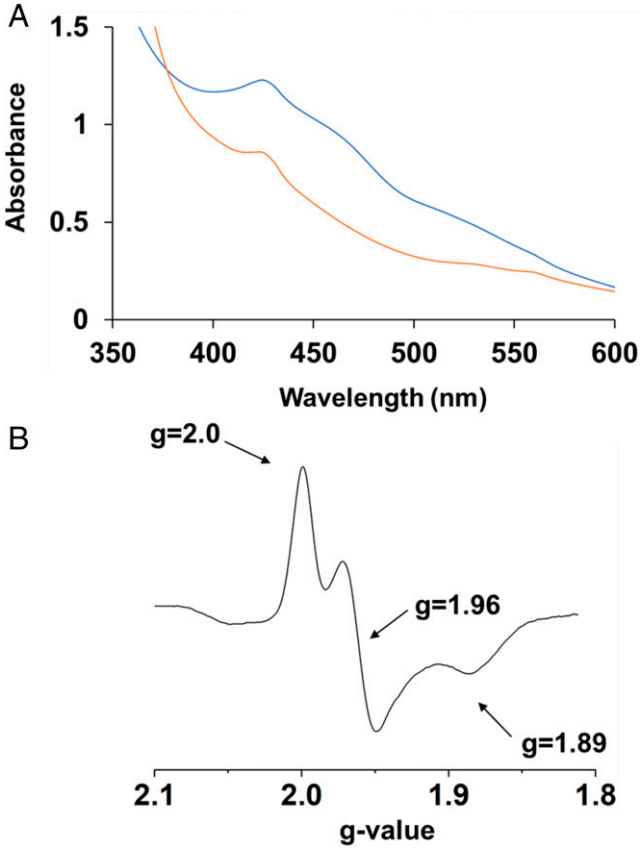

Fig. 4. (*A*) The presence of a [2Fe-2S] cluster in an isolated XcbA (blue) is indicated by the observed ultraviolet-vis absorption bands near 420, 450, and 520 nm. Decreased absorption at 420 nm was observed after the addition of dithionite (orange), suggesting dithionite can reduce XcbA. (*B*) The X-band EPR spectrum of 100 μM XcbA with 2 mM added dithionite. The measured *g*-values are reminiscent of previously characterized [2Fe-2S] ferredoxin (46).

internal aldimine facilitates the concerted decarboxylation reaction and release of sulfoethanethioaldehyde and either alanine or pyruvate + ammonia. We have further shown that the unique protein XcbA possesses a [2Fe-2S] cluster enzyme and is capable of undergoing oxidation-reduction and catalyzes the reduction of sulfoethanethioaldehyde to form CoM.

We have revealed that CoM biosynthesis in bacteria occurs by a suite of enzymes that are distinct from those involved in the CoM biosynthetic pathways found in methanogenic archaea, indicating that biosynthesis of this cofactor in bacteria and archaea evolved independently. As is the case with many methanogen genes (38), genes encoding enzymes in the CoM biosynthesis pathway in methanogens have low similarity in amino acid sequence to any biochemically characterized proteins (13, 14). As revealed here, the CoM biosynthesis pathway in bacteria is composed of enzymes from known families, such as AFS- and PLP-dependent enzymes, likely reflecting the attributes of the evolution of a more modern biochemical pathway. In conclusion, the elucidation of the biosynthetic pathway in bacteria reveals that the biosynthesis of CoM in bacteria and archaea represents a profound case of convergent evolution (39, 40).

Materials and Methods

Cloning of *xcbA-E*. *xcbA* (XAUT_RS25610) was amplified by PCR with the Phusion High-Fidelity DNA Polymerase enzyme (ThermoFisher Scientific) using the following primers, *xcbA*-F: 5′-GGAATTC*CATATG*AATAAACCGGAAAAAATTGAACCGAAACCGATTGCCC-3′ and *xcbA2*-R: 5′-AATG*CCTAGG*TCAGTGGTGGTGGTGGTGGTGCTCGAGTGCGGCCGCAAGCTTCGAT-3′. NdeI and AvrII restriction sites (in italics above) were respectively inserted upstream and downstream of the start and the stop codons in the primer sequences. The amplified fragment was digested by NdeI and AvrII and cloned into the MCS1 of the pETDuet-1 ampicillin-resistant vector. *xcbB* (XAUT_RS24680) and *xcbE* (XAUT_RS24695) were cloned under the MCS1 of pETDuet-1 ampicillin-resistant vector and *xcbC* (XAUT_RS24685) was cloned under MCS1 of pACYCDuet-1 chloramphenicol-resistant vector, as described by Partovi et al. (15). In order to express *X. autotrophicus* XcbD as an N terminus His-tagged protein in *Escherichia coli*, *xcbD* (XAUT_RS24690) gene sequence was amplified from the pXAUT01 megaplasmid (15, 41, 42) and cloned into Duet Expression Systems (Novagen). *xcbD* was amplified by using the same strategy with the following primers, *xcbD*-F: 5′-CGC*GGATCC*ACTGGTTGGTCCTTTGGATCACGTATCTATGGAGGCGCATGGAGC-3′ and *xcbD*-F: 5′-CCC*AAGCTT*TCAGGCTGCTCCATCCCGCGCGCCT-3′. BamHI and HindIII restriction sites (in italics above) were respectively inserted upstream and downstream of the start and the stop codons in the primer sequences. The amplified fragment was digested by BamHI and HindIII and cloned into the MCS1 of the pRSFDuet-1 kanamycin-resistant vector. The resultant plasmid was verified by sequencing (Functional Biosciences).

Expression and Purification of XcbA-E. Expression of XcbA-E was adapted from a previous method (14). BL21(DE3) competent cells were transformed with each construct, *xcbA*-pETDuet-1, *xcbB*-pETDuet-1, *xcbC*-pACYCDuet-1, *xcbD*-pRSFDuet-1, and *xcbE*-pETDuet-1, and cells were grown on lysogeny broth (LB) agar plates supplemented with ampicillin (Amp) (0.1 mg/mL), or kanamycin (Kan) (0.05 mg/mL), respectively. A single colony was used to inoculate an overnight culture in liquid LB medium (150 mL), supplemented with Amp, Cam, or Kan medium. Expression was initiated with 10% volume of the overnight culture and incubated at 37 °C with shaking at 250 rpm until the culture reached an OD600 of 0.4–0.6. Protein expression was induced with 1 mM IPTG and the cells moved to a 30 °C incubator with shaking at 180 rpm. Protein expression proceeded for 12 h before the cells were harvested by centrifugation (5,000 rpm, 30 min) followed by flash freezing of the pellets in liquid nitrogen. For purification, XcbA, XcbD, and XcbE frozen cell pellets were resuspended in lysis buffer modified from a previously described procedure: 20 mM Tris, 500 mM NaCl, 5 mM imidazole, 5% glycerol, pH 8 (12). Cell pellets from cultures were lysed using a sonicator (Q700 Qsonica LLC). Lysates were cleared by centrifugation: 16,000 rpm for 30 min prior to fast protein liquid chromatography (FPLC, Bio-Rad). Ni-NTA columns were equilibrated to the lysis buffer prior to loading the cleared lysate. For FPLC elution, 100% lysis buffer was run for 30 min and then a gradient from 0 to 100% elution buffer was applied over 10 min. The elution buffer for XcbA, XcbD, and XcbE contained: 20 mM Tris, 500 mM NaCl, 300 mM imidazole, and 10% glycerol. SDS-PAGE and Western blot anti-His tag antibodies (alkaline phosphatase conjugated monoclonal immunoglobulin, from hybridoma clone His-1 from Sigma) were used to determine the purity of the protein as well as integrity of the His-tag. Buffer exchange of the pure protein into imidazole-free buffer (20 mM Tris pH 8, 100 mM NaCl) was carried out via centrifuge filtration on 30 kDa filters (Millipore Sigma) as a final step prior to storage at −80 °C in 10% glycerol.

Detection of Phosphosulfolactate Production from XcbB Catalyzed Reaction. To produce phosphosulfolactate, 1 mM of phosphoenol pyruvate (PEP) and 1 mM of sodium bisulfite was dissolved in the buffer that contains 1 mM Tris, 1 mM NaCl, pH 8 in a final volume of 300 μL. The reaction was initiated by adding 0.5 mg of XcbB enzyme. The reaction was incubated for 1 h at 30 °C, followed by quench with molecular weight cutoff filtration. The detection of phosphosulfolactate was performed by using a 1290 series HPLC and 6530 series Q-TOF MS (Agilent) equipped with an electrospray ionization source (operated in negative polarity mode). The Q-TOF MS codition are as followed: Capillary was at 3.5 kV; the sampling cone was at 65 V; the source was at 325 °C; the sheath gas temperature was 350 °C; and drying gas and sheath gas flow were at 10 and 11 L min^{-1}. Fragmentation was carried out in a data-independent mode using a collision energy ramp of 15–50 eV. Analytes were directly injected to Q-TOF MS. Data were analyzed with MassHunter software version B.04.00 (Agilent).

Detection of Sulfoacrylic Acid from XcbC Activity. Phosphosulfolactate produced by XcbB was used as the substrate for XcbC. Enzymatic assays were conducted with 5 mM PEP, 5 mM sodium bisulfite, and 0.5 mg of XcbB in the buffer that contains (1 mM Tris, 1 mM NaCl, pH 8). The reaction is incubated for 1 h at 30 °C, followed by quench with molecular weight cutoff filtration. To the supernatant, 0.5 mg of XcbC was added to begin the consumption of phosphosulfolactate. Reactions were incubated for 3 h at 30 °C and quenched as XcbB reaction. The detection of sulfoacrylic acid was performed by using liquid chromatography mass spectrometry. A Synapt G2-S equipped with an Acquity system and photodiode array detector (Waters) was used for UPLC-QTOF-MS analysis. Analytes were separated on an Acquity HSS T3 UPLC column (length, 100 mm; diameter, 2.1 mm; particle size, 1.8 μm) using acetonitrile with 0.1% formic acid as solvent B and water with 0.1% formic acid as solvent A at a flow rate of 200 μL min^{-1} and the following linear gradient extending over 14 min: 0.0 min, 2% B; 5.0 min, 2% B, 7.0 min: 45% B; 7.5 min, 55% B; 8.0 min: 95% B, 11.0 min: 95% B, and 11.5 min: 2% B held till end of run. 2 μL of sample were loaded onto the column. The column temperature was kept at 40 °C while the samples were at 8 °C. Mass spectra were collected in negative continuum electrospray ionization mode over a range of *m/z* 50 to 1,200 with a scan time of 0.2 s. The capillary was at 2.5 kV. The sampling cone was at 40 V. The source was at 100 °C. The desolvation temperature was at 250 °C. Cone gas and desolvation gas flow were at 0 and 850 L h^{-1}. Fragmentation was carried out in a data-independent mode using a collision energy ramp of 15–50 eV. The mass spectrometer was calibrated using sodium formate with an accuracy cutoff of 1 ppm. LeucineEnkephalin was infused throughout the run and used for postacquisition mass correction. Data evaluations were performed using MassLynx 4.1 and integrated modules (Waters).

Determination of 3-Sulfo Propionyl Cysteine Production from XcbD Activity. Enzymatic assays were conducted with 250 μL reaction buffer (20 mM potassium phosphate, 10 mM NaCl, pH 8), 5 mM cysteine, and 5 mM synthetic sulfoacrylic acid (*SI Appendix*, Scheme S1). XcbD (0.5 mg) was injected to initiate the reaction (43). Reactions were incubated for 3 h at 30 °C, followed by quench with molecular weight cutoff filtration. The detection of 3-sulfo propionyl cysteine was performed by using UPLC-QTOF-MS and was adapted from the method of sulfoacrylic acid detection.

Detection of Sulfoethanethioaldehyde Production from XcbE Activity. 3-Sulfo propionyl cysteine produced by XcbD was used as the substrate for XcbE in a coupled reaction. The sample containing 20 mM potassium phosphate,

10 mM NaCl, pH 8, 5 mM cysteine, 5 mM sulfoacrylic acid, 0.5 mg of XcbD, and distilled H_2O in a final volume of 300 μL was incubated for 3 h at 30 °C, followed by quench with 50 K molecular weight cutoff filtration. To the filtrate, 0.5 mg of XcbE was added to start the consumption of 3-sulfo propionyl cysteine. The reaction was quenched with 30K molecular weight cutoff filtration after 3 h incubation at 30 °C. The method was adapted from the same method described above for the detection of sulfoethanethioaldehyde by LC-MS.

Determining the Production of CoM by the XcbA Catalyzed Reaction. Sulfoethanethioaldehyde produced by XcbE was used as the substrate for XcbA. After the completion of XcbE reaction, the reaction was quenched with the 30 K molecular weight cutoff filtration. XcbA was added and the reaction was incubated for 3 h at 30 °C, followed by quench with 30K molecular weight cutoff filtration. The resulting product was concentrated to 100 μL by speed vacuum and then derivatized by adding 10 μL of 1% tri(N)-butylphosphine (TBP) in 2-propanol, 20 μL of ethanolamine (20 μL/mL of boric acid buffer at pH 9), and 20 μL of *o*-phthalaldehyde (20 mg/mL of methanol). Samples were allowed to derivatize aerobically for 5 min at room temperature (44) (*SI Appendix*, Fig. S12). The detection of derivatized CoM was performed by using the same method described for phosphosulfolactate detection by HPLC-QTOF-MS. Analytes were separated on a Luna C18 column (length, 150 mm; diameter, 4.6 mm; particle size, 5 μm) using water with 0.1% formic acid as solvent A and acetonitrile with 0.1% formic acid as solvent B, run isocratically at 70% solvent A for 15 min at a flow rate of 1 mL min^{-1}. Data were analyzed with MassHunter software version B.04.00 (Agilent).

Time-Resolved ^{1}H NMR Spectroscopy. Time-resolved ^{1}H-NMR experiments were performed using a 600-MHz Varian NMR spectrometer. Samples were prepared by first adding 250 μL reaction buffer (20 mM potassium phosphate, 10 mM NaCl, pH 8, in D_2O), 5 mM cysteine, and 5 mM sulfoacrylic acid, followed by an initial scan to determine baseline peaks. XcbD (0.5 mg) was injected to initiate the reaction and monitored over the course of 3 h with NMR experiments every 5 min. 1D ^{1}H NMR spectra were acquired with 128 scans and a spectral width of 12 ppm (45). Spectral processing and analysis were performed using the Mnova 14 software (Mestrelab). Approximately 0.5 mg of XcbE was added to the reaction upon completion of the XcbD time course. The reaction was again monitored over 3 h with scans every 5 min as above.

EPR Spectroscopy. The X-band EPR spectrum of 100 μM XcbA with 2 mM added dithionite was measured at 0.53 mW microwave power, 100 kHz modulation frequency, and 10 G modulation amplitude, 15K, pH 8.0. The measured *g*-values are reminiscent of a plant-type [Fe_2S_2] cluster coordinated by two inorganic sulfides and two cysteine residues. X-band continuous wave EPR spectra were measured with a Bruker EMX spectrometer fitted with a ColdEdge (Sumitomo Cryogenics) waveguide in-cavity cryogen-free system with an Oxford Mercury iTC controller unit and helium Stinger recirculating unit (Sumitomo Cryogenics, ColdEdge Technologies). Helium gas flow was maintained at 100 psi.

Data, Materials, and Software Availability. All study data are included in the article and/or *SI Appendix*.

ACKNOWLEDGMENTS. This work was supported by the US Department of Energy (DOE), Office of Science, Office of Basic Energy Sciences (Award DE-SC0018143 to J.W.P. and J.L.D.). Partial salary support for J.W.P. and B.M.L. was provided by the United States Department of Agriculture National Institute of Food and Agriculture (Hatch Umbrella Project 15621). Support for Washington State University's NMR Center has been provided by the M.J. Murdock Charitable Trust (SR-201912845) and by private donors Don and Marianna Matteson. The content is solely the responsibility of the authors and does not necessarily represent the official views of the funding agencies. This work was authored in part by Alliance for Sustainable Energy, LLC, the manager and operator of the National Renewable Energy Laboratory for the DOE under Contract DE-AC36-08GO28308. Funding was provided to C.E.W. and C.E.L. by the US DOE Office of Science Early Career Program. The views expressed in the article do not necessarily represent the views of the DOE or the US government. The US government and the publisher, by accepting the article for publication, acknowledges that the US government retains a nonexclusive, paid-up, irrevocable, worldwide license to publish or reproduce the published form of this work, or allow others to do so, for US government purposes.

Author affiliations: [a]Institute of Biological Chemistry, Washington State University, Pullman, WA 99164; [b]Department of Chemistry, Washington State University, Pullman, WA 99164; [c]Biosciences Center, National Renewable Energy Laboratory, Golden, CO 80401; [d]Department of Chemistry and Biochemistry, Montana State University, Bozeman, MT 59717; and [e]M.J. Murdock Metabolomics Laboratory, Washington State University, Pullman, WA 99164

1. B. C. McBride, R. S. Wolfe, A new coenzyme of methyl transfer, coenzyme M. *Biochemistry* **10**, 2317–2324 (1971).
2. T. Wongnate *et al.*, The radical mechanism of biological methane synthesis by methyl-coenzyme M reductase. *Science* **352**, 953–958 (2016).
3. S. Scheller, M. Goenrich, R. Boecher, R. K. Thauer, B. Jaun, The key nickel enzyme of methanogenesis catalyses the anaerobic oxidation of methane. *Nature* **465**, 606–608 (2010).
4. C. D. Taylor, B. C. McBride, R. S. Wolfe, M. P. Bryant, M. Coenzyme, Coenzyme M, essential for growth of a rumen strain of Methanobacterium ruminantium. *J. Bacteriol.* **120**, 974–975 (1974).
5. W. E. Balch, R. S. Wolfe, Specificity and biological distribution of coenzyme M (2-mercaptoethanesulfonic acid). *J. Bacteriol.* **137**, 256–263 (1979).
6. R. Wolfe, "Novel coenzymes of archaebacteria" in *The Molecular Basis of Bacterial Metabolism*, G. Hauska, R. K. Thauer, Eds.(Springer, Berlin, Heidelberg, 1990), pp. 1–12.
7. A. Gendron, K. D. Allen, Overview of diverse methyl/alkyl-coenzyme M reductases and considerations for their potential heterologous expression. *Front. Microbiol.* **13**, 867342 (2022).
8. R. Laso-Pérez *et al.*, Thermophilic archaea activate butane via alkyl-coenzyme M formation. *Nature* **539**, 396–401 (2016).
9. R. Singh, M. S. Guzman, A. Bose, Anaerobic oxidation of ethane, propane, and butane by marine microbes: A mini review. *Front. Microbiol.* **8**, 2056 (2017).
10. F. Mus *et al.*, Insights into the unique carboxylation reactions in the metabolism of propylene and acetone. *Biochem. J.* **477**, 2027–2038 (2020).
11. J. R. Allen, D. D. Clark, J. G. Krum, S. A. Ensign, A role for coenzyme M (2-mercaptoethanesulfonic acid) in a bacterial pathway of aliphatic epoxide carboxylation. *Proc. Natl. Acad. Sci. U.S.A.* **96**, 8432–8437 (1999).
12. A. M. Krishnakumar *et al.*, Getting a handle on the role of coenzyme M in alkene metabolism. *Microbiol. Mol. Biol. Rev.* **72**, 445–456 (2008).
13. D. E. Graham, M. Graupner, H. Xu, R. H. White, Identification of coenzyme M biosynthetic 2-phosphosulfolactate phosphatase. A member of a new class of Mg(2+)-dependent acid phosphatases. *Eur. J. Biochem.* **268**, 5176–5188 (2001).
14. D. E. Graham, R. H. White, Elucidation of methanogenic coenzyme biosyntheses: From spectroscopy to genomics. *Nat. Prod. Rep.* **19**, 133–147 (2002).
15. S. E. Partovi *et al.*, Coenzyme M biosynthesis in bacteria involves phosphate elimination by a functionally distinct member of the aspartase/fumarase superfamily. *J. Biol. Chem.* **293**, 5236–5246 (2018).
16. D. E. Graham, S. M. Taylor, R. Z. Wolf, S. C. Namboori, Convergent evolution of coenzyme M biosynthesis in the Methanosarcinales: Cysteate synthase evolved from an ancestral threonine synthase. *Biochem. J.* **424**, 467–478 (2009).
17. I. Anderson *et al.*, Genomic characterization of methanomicrobiales reveals three classes of methanogens. *PLoS One* **4**, e5797 (2009).
18. D. E. Graham, H. Xu, R. H. White, Identification of coenzyme M biosynthetic phosphosulfolactate synthase: A new family of sulfonate-biosynthesizing enzymes. *J. Biol. Chem.* **277**, 13421–13429 (2002).
19. E. L. Wise, D. E. Graham, R. H. White, I. Rayment, The structural determination of phosphosulfolactate synthase from Methanococcus jannaschii at 1.7-A resolution: An enolase that is not an enolase. *J. Biol. Chem.* **278**, 45858–45863 (2003).
20. M. Graupner, H. Xu, R. H. White, Identification of an archaeal 2-hydroxy acid dehydrogenase catalyzing reactions involved in coenzyme biosynthesis in methanoarchaea. *J. Bacteriol.* **182**, 3688–3692 (2000).
21. M. Graupner, H. Xu, R. H. White, Identification of the gene encoding sulfopyruvate decarboxylase, an enzyme involved in biosynthesis of coenzyme M. *J. Bacteriol.* **182**, 4862–4867 (2000).
22. S. A. Ensign, M. R. Hyman, D. J. Arp, Cometabolic degradation of chlorinated alkenes by alkene monooxygenase in a propylene-grown Xanthobacter strain. *Appl. Environ. Microbiol.* **58**, 3038–3046 (1992).
23. X. Liu, T. E. Mattes, Epoxyalkane: Coenzyme M transferase gene diversity and distribution in groundwater samples from chlorinated-ethene-contaminated sites. *Appl. Environ. Microbiol.* **82**, 3269–3279 (2016).
24. J. G. Krum, S. A. Ensign, Heterologous expression of bacterial Epoxyalkane:Coenzyme M transferase and inducible coenzyme M biosynthesis in Xanthobacter strain Py2 and Rhodococcus rhodochrous B276. *J. Bacteriol.* **182**, 2629–2634 (2000).
25. C. G. van Ginkel, H. G. Welten, J. A. de Bont, Oxidation of gaseous and volatile hydrocarbons by selected alkene-utilizing bacteria. *Appl. Environ. Microbiol.* **53**, 2903–2907 (1987).
26. J. G. Krum, S. A. Ensign, Evidence that a linear megaplasmid encodes enzymes of aliphatic alkene and epoxide metabolism and coenzyme M (2-mercaptoethanesulfonate) biosynthesis in Xanthobacter strain Py2. *J. Bacteriol.* **183**, 2172–2177 (2001).
27. V. Puthan Veetil, G. Fibriansah, H. Raj, A.-M. W. Thunnissen, G. J. Poelarends, Aspartase/fumarase superfamily: A common catalytic strategy involving general base-catalyzed formation of a highly stabilized aci-carboxylate intermediate. *Biochemistry* **51**, 4237–4243 (2012).
28. B. Van Laer *et al.*, Molecular comparison of Neanderthal and modern human adenylosuccinate lyase. *Sci. Rep.* **8**, 18008 (2018).
29. S. R. Bharath, S. Bisht, R. K. Harijan, H. S. Savithri, M. R. N. Murthy, Structural and mutational studies on substrate specificity and catalysis of Salmonella typhimurium D-cysteine desulfhydrase. *PLoS One* **7**, e36267 (2012).
30. A. Hoegl *et al.*, Mining the cellular inventory of pyridoxal phosphate-dependent enzymes with functionalized cofactor mimics. *Nat. Chem.* **10**, 1234–1245 (2018).

31. K. R. Dixon, M. Fakley, A. Pidcock, Solvent, concentration, and temperature dependance of the platinum–phosphorus nuclear magnetic résonance coupling constants in cis-and trans- [PtCl2 (PBu3 n) 2]. *Can. J. Chem.* **54**, 2733–2738 (1976).
32. Z. Chen, T. Hou, Z.-W. Chen, D. W. Hwang, L.-P. Hwang, Selective intermolecular zero-quantum coherence in high-resolution NMR under inhomogeneous fields. *Chem. Phys. Lett.* **386**, 200–205 (2004).
33. C. Faber, E. Pracht, A. Haase, Resolution enhancement in in vivo NMR spectroscopy: Detection of intermolecular zero-quantum coherences. *J. Magn. Reson.* **161**, 265–274 (2003).
34. W. M. McGregor, D. C. Sherrington, Some recent synthetic routes to thioketones and thioaldehydes. *Chem. Soc. Rev.* **22**, 199–204 (1993).
35. A. P. Landry, H. Ding, Redox control of human mitochondrial outer membrane protein MitoNEET [2Fe-2S] clusters by biological thiols and hydrogen peroxide. *J. Biol. Chem.* **289**, 4307–4315 (2014).
36. L. Aymé *et al.*, Arabidopsis thaliana DGAT3 is a [2Fe-2S] protein involved in TAG biosynthesis. *Sci. Rep.* **8**, 17254 (2018).
37. S. Dai *et al.*, Structural snapshots along the reaction pathway of ferredoxin-thioredoxin reductase. *Nature* **448**, 92–96 (2007).
38. J. G. Ferry, Methane: Small molecule, big impact. *Science* **278**, 1413–1414 (1997).
39. R. S. Nett *et al.*, Elucidation of gibberellin biosynthesis in bacteria reveals convergent evolution. *Nat. Chem. Biol.* **13**, 69–74 (2017).
40. K. Heyduk, J. J. Moreno-Villena, I. S. Gilman, P.-A. Christin, E. J. Edwards, The genetics of convergent evolution: Insights from plant photosynthesis. *Nat. Rev. Genet.* **20**, 485–493 (2019).
41. W. Vishniac, M. Santer, The thiobacilli. *Bacteriol. Rev.* **21**, 195–213 (1957).
42. W. M. Wiegant, J. A. De Bont, A new route for ethylene glycol metabolism in Mycobacterium E44. *Microbiology* **120**, 325–331 (1980).
43. Y. Joyard, C. Papamicaël, P. Bohn, L. Bischoff, Synthesis of sulfonic acid derivatives by oxidative deprotection of thiols using tert-butyl hypochlorite. *Org. Lett.* **15**, 2294–2297 (2013).
44. D. A. Elias, L. R. Krumholz, R. S. Tanner, J. M. Suflita, Estimation of methanogen biomass by quantitation of coenzyme M. *Appl. Environ. Microbiol.* **65**, 5541–5545 (1999).
45. S. J. Ullrich, U. A. Hellmich, S. Ullrich, C. Glaubitz, Interfacial enzyme kinetics of a membrane bound kinase analyzed by real-time MAS-NMR. *Nat. Chem. Biol.* **7**, 263–270 (2011).
46. R. Cammack, E. Gay, J. K. Shergill, Studies of hyperfine interactions in [2Fe-2S] proteins by EPR and double resonance spectroscopy. *Coord. Chem. Rev.* **190–192**, 1003–1022 (1999).